PAPER Special Section on Photonic Crystals and Their Device Applications

Finite-Difference Time-Domain Simulation of Two-Dimensional Photonic Crystal Surface-Emitting Laser Having a Square-Lattice Slab Structure

Mitsuru YOKOYAMA[†,††,†††a)], *Nonmember and* Susumu NODA[†,†††], *Member*

SUMMARY By means of the three-dimensional (3D) finite-difference time domain (FDTD) method, we have investigated in detail the optical properties of a two-dimensional photonic crystal (PC) surface-emitting laser having a square-lattice structure. The 3D-FDTD calculation is carried out for the finite size PC slab structure. The device is based on band-edge resonance, and plural band edges are present at the corresponding band edge point. For these band edges, we calculate the mode profile in the PC slab, far field pattern (FFP) and polarization mode of the surface-emitted component, and photon lifetime. FFPs are shown to be influenced by the finiteness of the structure. Quality (Q) factor, which is a dimensionless quantity representing photon lifetime, is introduced. The out-plane radiation loss in the direction normal to the PC plane greatly influences the total Q factor of resonant mode and is closely related with the band structure. As a result, Q factors clearly differ among these band edges. These results suggest that these band edges include resonant modes that are easy to lase and resonant modes that are difficult to lase.

key words: *photonic crystal, semiconductor surface-emitting laser, finite-difference time-domain simulation, far field pattern, quality factor*

1. Introduction

Light waves in a material having a periodic refractive index change exhibit either a unique dispersion relation or a band structure similar to an electron wave inside a solid-state crystal. Such a band structure is called a photonic band, and a new optical material exhibiting this property, called a photonic crystal (PC), can arbitrarily control light propagation and/or emission and has attracted much attention in recent years [1]–[5]. Unique devices that have been reported are based on various engineering techniques, such as defect engineering, band-edge engineering, and band engineering [6]. Among these, band-edge engineering can be utilized to realize a unique semiconductor laser. Standing waves formed at each band edge of the photonic band structure are used as laser cavities [7]–[13]. In previous studies, we reported a surface-emitting laser having a two-dimensional (2D) PC and demonstrated the coherent lasing action. A single longitudinal and/or lateral mode oscillation was successfully achieved over a large area [7], [8]. We also demonstrated polarization mode control in a 2D square-lattice PC laser by controlling the geometry of the unit cell structure [9], [10]. In these studies we used the above-mentioned band edge for formation of the standing wave and thus the 2D cavity mode. Among the band edges in the band structure, we utilize the folded (second order) Γ point toward the Γ-X direction (Γ2 point). This band edge induces not only in-plane optical coupling, but also diffraction in the direction normal to the PC surface. As a result, the device functions as a surface-emitting laser. In the case of the square-lattice PC discussed in this paper, four band edges are present at the band edge of the Γ2 point. However, whether these four band edges differ in resonant mode characteristics, such as profiles and polarization of a surface-emitting component and photon lifetime, remains unclear.

In this paper, we report characteristics of resonant modes at band edges of the Γ2 point in a PC of finite size. We use the finite-difference time-domain (FDTD) method to calculate the mode profile, far field pattern (FFP), polarization mode, and photon lifetime. The FDTD method is a widely used numerical technique for solving Maxwell's equations [14], [15]. It can determine optical phenomena in a complex photonic structure such as a PC. In Sect. 2, we describe the calculation method for the resonant mode in the 2D PC. In Sect. 3, we describe the calculation results of resonant mode in detail. We show the band structure, mode profile, FFP, and polarization of the surface-emitted component. Next, quality (Q) factor, which is a dimensionless quantity representing photon lifetime, is introduced. We show that the out-plane radiation loss in the direction normal to the PC plane greatly influences the total Q factor in the case of the resonant mode at the Γ2 point and that it is closely related to the band structure. As a result, Q factors are proven to differ depending on band edges of the Γ2 point.

2. Calculation Model and Method

In this section, we explain the calculation method. We consider the 2D square-lattice PC slab, having a circular unit cell structure. Figure 1 shows the model used for the 3D FDTD calculation. The 2D PC is formed in a dielectric slab having a dielectric constant ε_b of 11.5 and a thickness of 0.24 μm (or 0.6a, where a is the lattice constant.), containing circular air rods ($\varepsilon_a = 1$). The air rods are arranged in

Manuscript received October 8, 2003.
Manuscript revised November 21, 2003.

[†]The authors are with the Department of Electronic Science and Engineering, Kyoto University, Kyoto-shi, 615-8510 Japan.
[††]The author is with Device Technology R&D Laboratories, Konica Minolta Technology Center Inc., Takatsuki-shi, 569-8503 Japan.
[†††]The authors are with Core Research for Evolutional Science and Technology (CREST), Japan Science and Technology Corporation (JST), Kyoto-shi, 615-8510 Japan.
a) E-mail: mitsuru.yokoyama@konicaminolta.jp

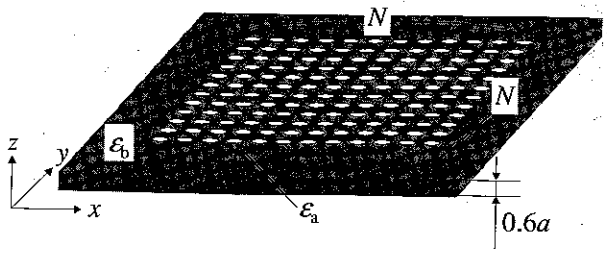

Fig. 1 Schematic of 3D-FDTD calculations. 2D photonic crystal slab consists of two dielectric materials; a background ($\varepsilon_b = 11.5$) and circular rods ($\varepsilon_a = 1$). Slab thickness is $0.6a$. The area fraction occupied by the air rod is 0.2 per unit cell. The cladding layers above and below the slab are air. N is the number of air rods in the Γ-X direction, and total number of air rods in the calculation region is N^2.

a square region as shown in Fig. 1. The area fraction occupied by the air rod is 0.2 per unit cell. The cladding layers above and below the slab are air. Mur's second-order absorbing boundary condition is employed. In order to estimate the resonant frequency at the corresponding band edge, the photonic band structure is also calculated by the 3D-FDTD method. For this calculation, Bloch's and Mur's second-order absorbing boundary conditions are employed for the horizontal and vertical boundary conditions, respectively. The parameters used in the FDTD calculation are $\Delta x = \Delta y = \Delta z = 1/10a$, and $\Delta t = 0.5\Delta x/c$, where c is the speed of light in a vacuum.

First, we calculate the band structure and estimate the $\Gamma 2$ band edge frequency for a structure of infinite size. We also calculate the electromagnetic field at the band edge. Next, electromagnetic fields of a PC slab structure of finite size are excited by the resonant frequency of each band edge obtained by band calculation at the center of the 2D PC slab. The excited dipole has a Gaussian pulse of a relatively wide frequency bandwidth. In view that the resonant mode is almost a Bloch wave even in the case of a structure of finite size, the excited dipoles are placed periodically at antinodes according to the electromagnetic pattern of each band edge calculated by 3D-FDTD calculation for infinite size. We assume that the resonant mode at the band edges is a transverse-electric (TE)-like mode, because the device is supposed to lase in this mode. Next, the resonant frequency is calculated by Fourier transform of the time-evolved field. The resonant frequency calculated by this method differs slightly from the resonant frequency of a structure of infinite size. Therefore, we re-excite by the resonant frequency obtained by calculation for the structure of finite size. Because the frequency separation among individual modes in the band edges of $\Gamma 2$ point is small, the excitation Gaussian pulse should have a narrow frequency bandwidth so as not to excite other neighboring band edges. However, a Gaussian pulse which has too narrow frequency bandwidth results in the Q factor of the structure being determined by the excitation pulse width itself. We pay close attention to the excitation pulse width.

Far Field Pattern (FFP) of the surface-emitting component is observed in the plane parallel to the slab at a distance of $40a$ from the surface of the PC slab. FFP is calculated by integrating the Poynting vector normal to the observational plane within a proper time range. Polarization of the FFP is evaluated by sampling the electric field at the observational plane. Here, we note that the FFP calculated by this method does not correspond to the FFP after lasing oscillation. In view that the linewidth of the spectrum after lasing oscillation is much more narrow than that determined by the cavity mode considered here, the FFP calculated by this method should be considered the FFP just before lasing oscillation. Meanwhile, Near Field Pattern (NFP) may also be interesting. However, NFP is difficult to define, because specifying the emitting surface of light is impossible. When the center of the slab is considered the emitting surface of light, the Poynting vector has no vertical component in relation to the slab, and therefore the profile cannot be calculated. When the surface of the slab is considered the emitting surface, the vertical component of the Poynting vector can be calculated. However, the evanescent component is dominant in this region, and therefore the Poynting vector is not sensible. Considering the inverse Fourier transform of FFP the NFP may be a good method. However, this requires detailed discussion, and we will report it elsewhere.

Three different methods can be used to calculate Q factor [16]. The first method is to determine Q factor from the linewidth of the resonant spectrum; the second method is to determine Q factor from the slope of the exponential decay of the stored energy vs. time relation, and the third method is to calculate the power absorbed in the boundary and divide the result by the energy stored in the structure. The first method is not preferable, because when Q factor is high, it requires a large number of time samples to calculate the Q factor precisely. The second and third methods can be considered equivalent for our study. We use the second method for calculating Q factor, but confirm that no discrepancy exists between Q factor calculated by the second method and Q factor calculated by the third method. To separate the loss of the guided mode in the PC slab and the out-plane radiation loss in the direction normal to the PC plane, we decompose the Q factor (Q_{total}) into horizontal Q factor ($Q_{//}$) and vertical Q factor ($Q_{\perp}$) [17].

3. Calculation Results

3.1 Band Structure and Field Distribution

In this section, we show the characteristics of resonant mode field distribution at the band edges. First, in Fig. 2 we show the band diagram near the $\Gamma 2$ point calculated by the 3D-FDTD method. Figure 2 shows that four bands (2nd, 3rd, 4th, and 5th Bands) exist, and that each band has a band edge (I, II, III, and IV) at the Γ point. Band edges III and IV are doubly degenerate and the other two are non-degenerate. The band structure calculated by the 3D-FDTD method is the same as that calculated by the 2D plane-wave expansion calculation in our previous work, except for shifted frequencies [9]. Next, we show the resonant field distributions of

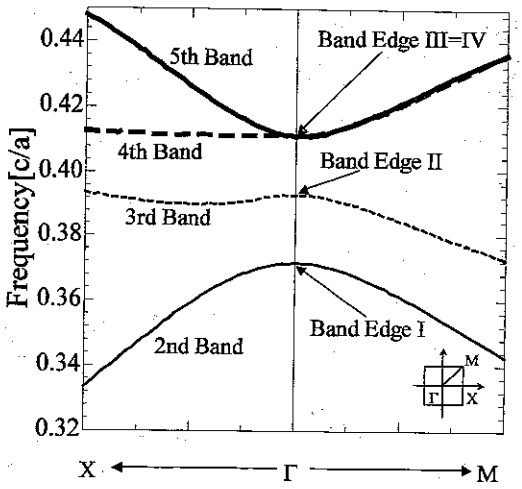

Fig. 2 Detailed band structure of square lattice photonic crystal slab around the Γ2 point for the transverse-electric (TE)-like mode, as calculated by the 3D-FDTD method.

finite size PC near the Γ2 point. Figure 3 shows the magnetic field distributions normal to the PC plane at the center of the PC slab. The number of air rods in the Γ-*X* direction (*N*) is 30. Figures 3(a) and (b) show the field distributions of band edges I and II, respectively. Due to the degeneracy, the field distributions of the band edges III and IV cannot be determined concretely, and thus cannot be shown in the figure. The rectangular region shown by a thin dotted line indicates the PC region. The insets of Fig. 3 are magnified field distributions near the center of the PC region, where thick black circles indicate the locations and shapes of lattice points. The field distributions indicated by the insets are consistent with those calculated by 2D plane-wave expansion calculation in our previous work, indicating that these resonant field distributions are caused by band edge resonance. In Fig. 3(a) magnetic field intensity decreases gradually toward the area surrounding the photonic crystal. In contrast, a beat pattern appears in magnetic field intensity in Fig. 3(b). The phenomenon may be understood when, as shown in Fig. 4, we show the wave number space (*k*-space) pattern of Fig. 3. Figure 4 is obtained by the Fourier transform of magnetic field of the PC area in Fig. 3. Strictly speaking, the *k*-space pattern should be obtained by the Fourier transform in both the spatial and time domains. However, the resonant modes of the band edges are considered to be almost standing wave states, even in the case of a structure of finite size. Therefore, the electromagnetic field is similar at every moment, except the moment of node in the standing wave state. Thus, we can consider the Fourier transform of field distribution in real space at the moment to be the *k*-space pattern. In order to obtain the *k*-space pattern precisely, attention should be paid to the influence of the window function when Fourier transform is carried out. In this paper, since the PC is arranged in a square region, we can minimize the influence of the window function. However, when the sampling number of area is not an integer power of 2, the *k*-space pattern is influenced by the window function when the Fast Fourier

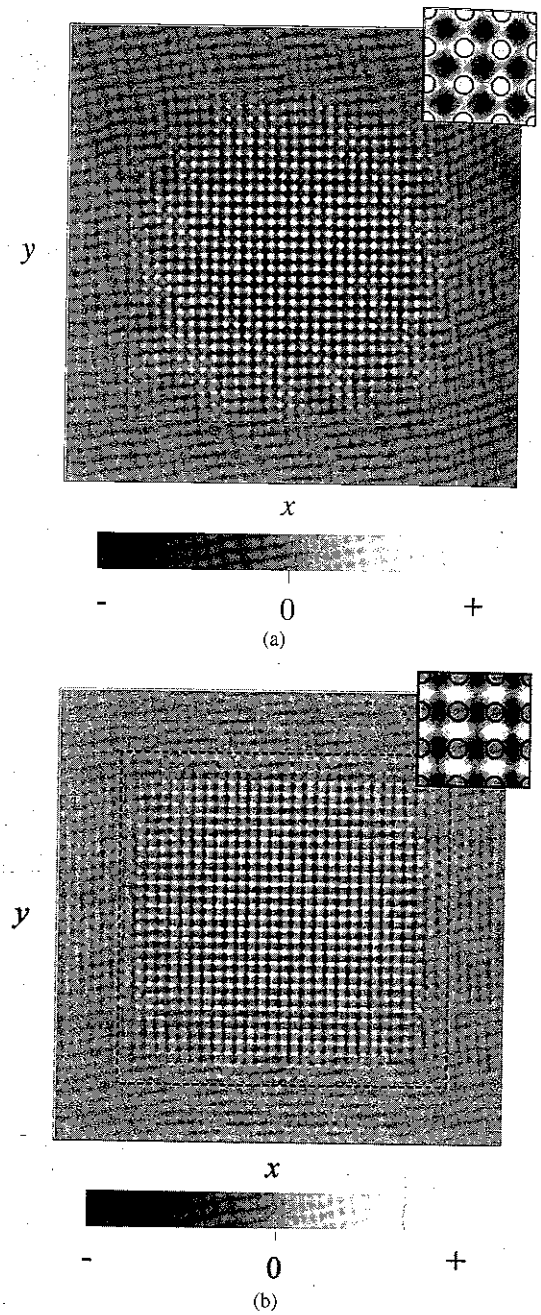

Fig. 3 Magnetic field distributions normal to the photonic crystal plane at the center of the photonic crystal slab. The number of air rods in the Γ-*X* direction (*N*) is 30. Figures 3(a) and (b) show the field distributions of band edges I and II, respectively.

Transform (FFT) is employed. Thus, in this work, we employ the Discreet Fourier Transform (DFT) in order to obtain the *k*-space pattern. The thin square dotted line in Fig. 4 represents the first Brillouin zone. The *k*-space pattern of resonant mode of the band edge I, as shown in Fig. 4(a), indicates that the wave number spreads in a certain region, but high intensity is present only around the Γ point. This is caused by finiteness of the structure; the wave number is not fixed securely at the Γ point and it spreads in a certain

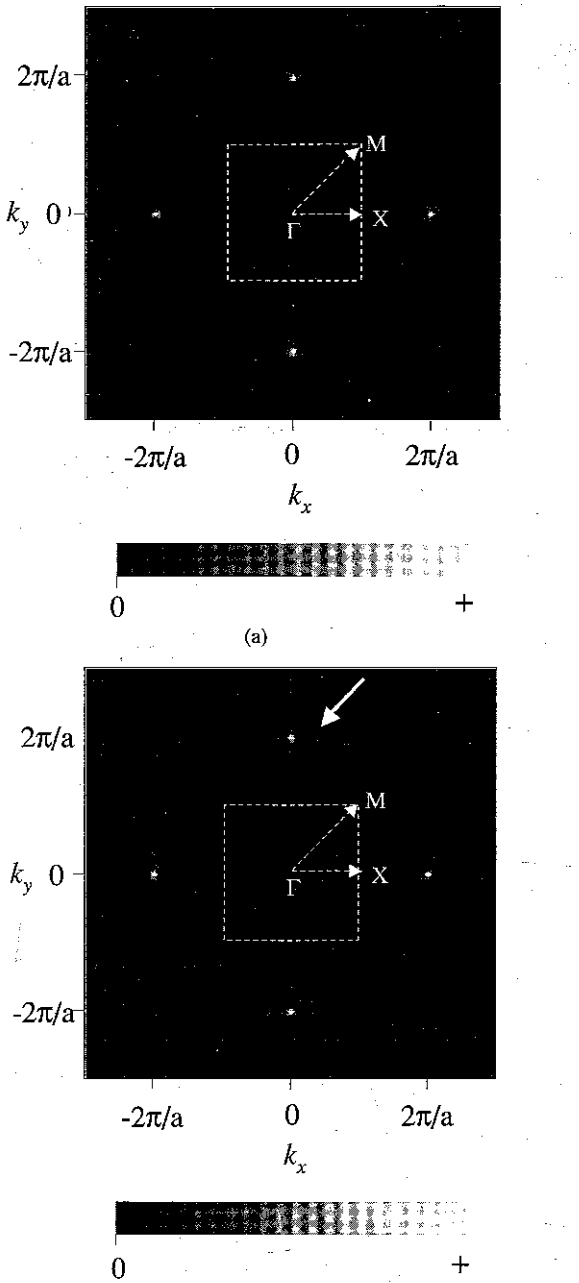

Fig. 4 The wave number space (k-space) patterns of Fig. 3. Figures 4(a) and (b) show the k-space pattern of the band edges I and II, respectively. The figures are obtained by the Fourier transform of magnetic field of the photonic crystal area shown in Fig 3. The thin square dotted line in Fig. 4 represents the first Brillouin zone.

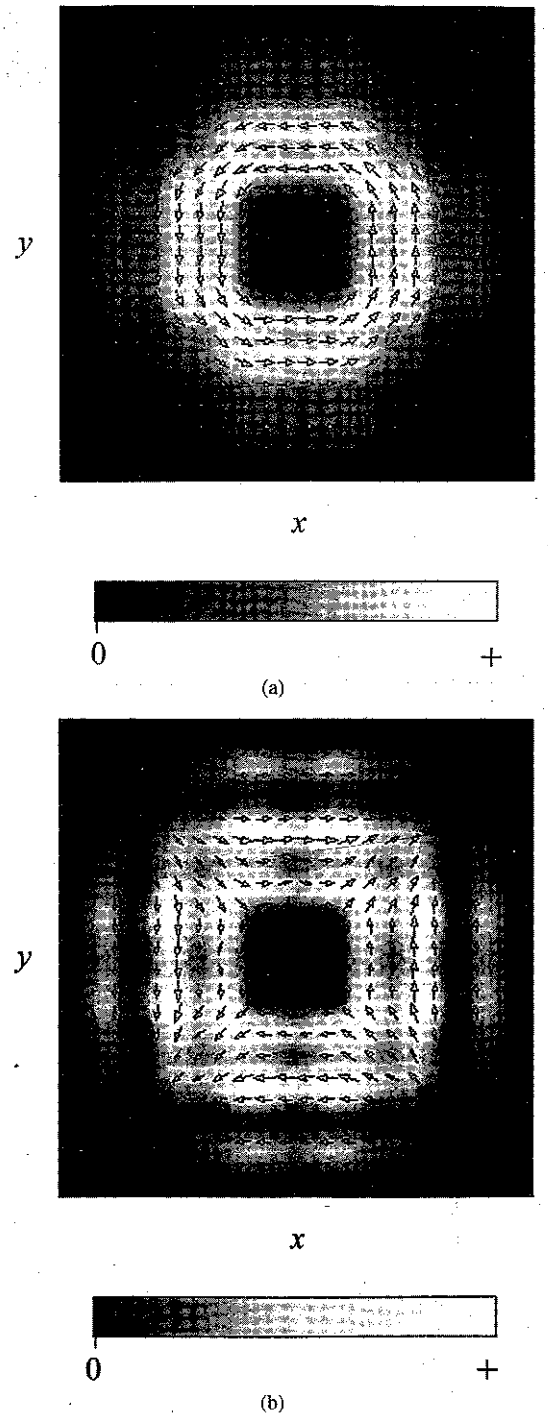

Fig. 5 (a) (b) Far field patterns (FFPs) of surface-emitted component of band edges I and II, respectively. Annular profiles having dark centers are obtained.

region around the Γ point. Meanwhile, the spread range of wave number in Fig. 4(b), which shows the k-space pattern of band edge II, is wider than that in Fig. 4(a). As indicated by the white arrow in Fig. 4(b), weak intensity spots other than the Γ points are present. The weak intensity spots are located a short distance from the Γ point in the Γ-X direction, and this is the reason for the beat pattern in magnetic field intensity seen in Fig. 3(b). These results can be understood from the shape of the band around the Γ2 point. In Fig. 2, the shape of the band around band edge I is upwardly convex, but that around band edge II is more complicated. The band toward the Γ-X direction around band edge II is flatter than that around band edge I. More specifically, in the Γ-X direction the frequency decreases and then increases. Hence, in the case of band edge II, the spread range of wave number becomes large, and the weak intensity spot shown

in Fig. 4(b) is the wave number that has the same energy at band edge II but a different wave number than at the Γ point. This wave number also influences the FFP of band edge II. Figures 5(a) and (b) show the FFP of band edges I and II, respectively. In Fig. 5 the white arrows indicate the local electric field; that is, the polarization direction of the FFP. Both the FFP of band edge I and that of band edge II show annular profiles. Here we note that the unit cell structure is circular, and the FFP of elliptical unit cell structure will be reported elsewhere. The reason for the annular profile is as follows. In a PC of infinite size, the eigen modes of band edges I and II do not couple to free space normal to the PC plane, because of symmetry mismatch [18], [19]. However, in a PC of finite size, wave number cannot be fixed securely to the Γ point, and spreads around the Γ point as shown in Fig. 4. In this case, the wave number shifted from Γ point can be coupled to free space, but the diffractive direction is slightly offset from the direction normal to the PC plane. As a result, we obtain an annular profile whose center is dark as shown in Fig. 5. The wave number exists discontinuously around the Γ point in the resonant mode of band edge II and the diffractive direction is complicated, resulting in the complicated FFP as shown in Fig. 5(b). This result influences the Q factor, as we will explain in the next section.

3.2 Quality Factors of Resonant Mode

First, Fig. 6 shows Q factors (Q_{total}) of Band edges I and II plotted against N. Q_{total} generally increases with N. However, the Q factor of band edge I is always larger than that of band edge II. A high Q factor as large as 5000 has been achieved for band edge I when N is 50. Meanwhile, for a given value of N, Q_{total} of band edge II is half Q_{total} of band edge I. In Fig. 2, the band around band edge II is flatter than that around band edge I. A flatter band edge is generally considered to have lower group velocity, and Q factor increases with decreasing group velocity. Hence, one may consider that a discrepancy exists between the calculated Q factor as shown in Fig. 6 and group velocity assumed from band structure. This phenomenon can be understood when we decompose Q_{total} into $Q_{//}$ and $Q_{\perp}$. Figure 7 shows $Q_{//}$ and $Q_{\perp}$ of Band edges I and II plotted against N. In the case of band edge I shown in Fig. 7(a), $Q_{\perp}$ is always larger than $Q_{//}$. In contrast, in the case of band edge II shown in Fig. 7(b), $Q_{//}$ is always larger than $Q_{\perp}$. However, the difference between band edges I and II in $Q_{//}$ is not very large. This is caused by the wave number spread around the Γ point when the structure is of finite size. As previously mentioned, wave number of band edge II spreads to a much greater extent than does that of band edge I. This is because band edge II is flatter than band edge I. If the wave number is fixed to the Γ point, no diffraction occurs normal to the PC plane, making $Q_{\perp}$ infinite. When the wave number is shifted from the Γ point, diffraction occurs normal to the PC plane, decreasing $Q_{\perp}$. When the wave number is shifted much further from the Γ point, the normal direction component of diffraction decreases, thereby increasing $Q_{\perp}$.

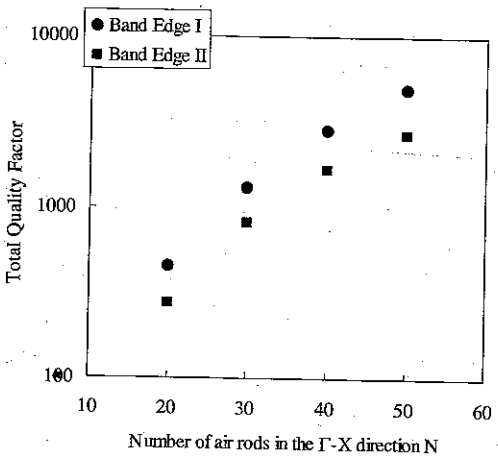

Fig. 6 Quality factor as a function of the number of air rods in the Γ-X direction for band edges I and II. Q factors generally increase with N. For a given value of N, the Q factor of band edge I is always larger than that of band edge II.

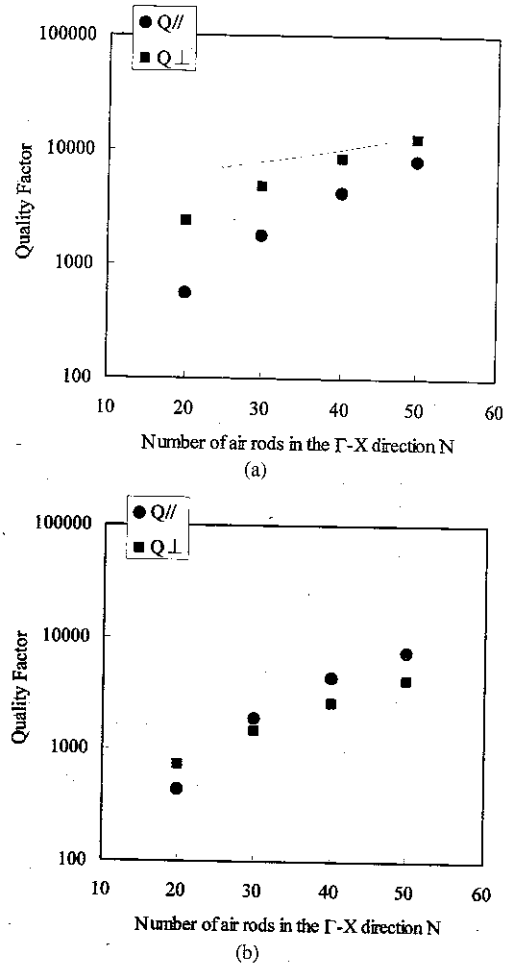

Fig. 7 (a) (b) Horizontal Q factor ($Q_{//}$) and vertical Q factor ($Q_{\perp}$) as a function of the number of air rods in the Γ-X direction for band edges I and II, respectively. $Q_{//}$ and $Q_{\perp}$ represent the out-plane radiation loss in the direction normal to the photonic crystal plane and $Q_{\perp}$ loss of guided mode in the photonic crystal slab, respectively.

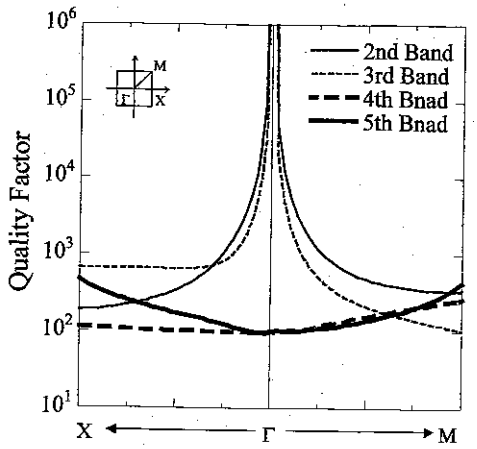

Fig. 8 Q factor of infinite size photonic crystal slab around the Γ2 point. Q factor is infinity at the Γ point for band edge I and band edge II, but Q factors of band edges III and IV are very small.

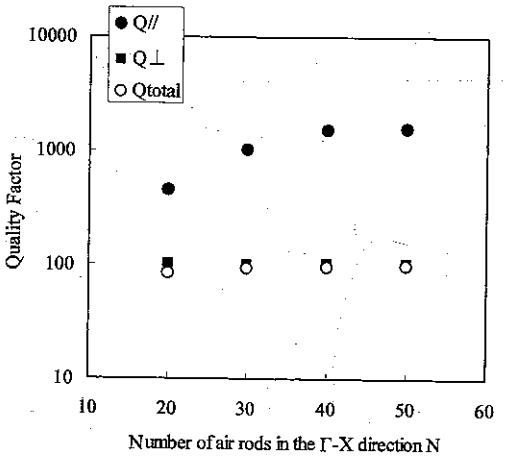

Fig. 9 Total Q factor (Q_{total}), horizontal Q factor ($Q_{//}$), and vertical Q factor ($Q_{\perp}$) as a function of the number of air rods in the Γ-X direction for band edges III and IV. Q_{total} is less than one-tenth Q_{total} of band edge I or II.

Thus, when the shape of band edge is flat, as in the case of band edge II, the spread range of wave number, which corresponds to the linewidth of the resonant spectrum determined by Q_{total}, becomes wide, and the resonant mode of the band edge become leaky. As a result, $Q_{\perp}$ decreases and Q_{total} decreases accordingly. In order to confirm this, Fig. 8 shows Q_{total} of an PC slab of infinite size around the Γ2 point. The total Q factor of infinite size is determined from the slope of the exponential decay of the stored energy in the infinite size structure discussed in Sect. 2 vs. time relation. When the structure size is infinite, $Q_{//}$ become infinite and Q_{total} is equal to $Q_{\perp}$. As expected, Q_{total} is infinite at the Γ point for band edge I and band edge II, but decreases drastically when the wave number is shifted from the Γ point. In contrast, band edges III and IV, which are essentially leaky [18], [19], show very small Q factor. Therefore, when the structure is of finite size, Q_{total} of band edges III and IV are considered to be small. Actually, as shown in Fig. 9, when we assume the proper electromagnetic field distribution for band edges III or IV and calculate the Q_{total} of a finite size structure, Q_{total} is confirmed to be less than one-tenth Q_{total} of band edge I or II. Even in this case, however, the decrease rate of $Q_{//}$ of band edge III or IV is not very large in comparison with that of band edges I and II. Therefore $Q_{//}$ may depend on structure size rather than on the band structure.

Recently, we carried out FDTD calculation on our actual manufactured device. The actual device is formed by an active layer sandwiched by p- and n-cladding layers [7]–[9]. The PC is embedded in the clad layer near the active layer. In this case, the difference in dielectric constant becomes small in comparison with the PC slab. The calculation results for the actual device suggest that the difference in Q factor among the band edges become small in comparison with the PC slab. Furthermore the device characteristics such as a FFP pattern will be modified when a phase shift is introduced to the PC or when the unit cell structure is properly designed. We will report these point elsewhere.

4. Conclusion

We have employed the 3D-FDTD method to calculate the mode profile in a PC slab, the surface-emitting components, and Q factors of the band edge resonant modes of a square-lattice PC slab of finite size. By exciting properly for the band structure, 3D-FDTD method is effective for analyzing the resonant mode of a PC structure of finite size. Both the FFP of band edge I and that of band edge II show an annular profile. This is because the wave number spreads in a certain region around the Γ point when the structure is of finite size. The wave number equal to the Γ point cannot couple to the free space, but that shifted from the Γ point can couple to the free space. From another viewpoint, both the electric field of the FFP of band edge I and that of band edge II show a whorled shape, and the electric fields interfere with each other at the center of the FFP, resulting in disappearance of the electric field at the center of the FFP, thereby yielding an annular profile whose center is dark.

We have also shown that 3D-FDTD is valid for calculation of Q factors of resonant mode. From the result of Q calculation, a high Q factor as large as 5000 for band edge I has been achieved in a structure whose number of air rods in the Γ-X direction (N) is 50. Meanwhile, for a given N value, Q factors of band edges II and III are one-half and one-fiftieth, respectively, the Q factor of band edge I. The reason why the Q factor of band edge II is small is that the spread range of wave number is wide, because of flatness of the band. Shifting the wave number from the Γ point causes decreases vertical Q factor ($Q_{\perp}$), resulting in a decrease of total Q factor. In contrast, the reason why the Q factors of band edges III or IV are small is that the eigen mode of band edge III or IV is essentially leaky, because of mode symmetry. These results suggest that the resonant mode of band edge I is relatively easy to lase.

Our recent calculations for our actual manufactured device suggest that the difference in Q factor among the band

edges become small in comparison with the PC slab. It has been also pointed out that by introducing the phase shift to the PC or by designing the unit cell structure properly, we can modify or improve device characteristics.

References

[1] E. Yablonovitch, "Inhibited spontaneous emission in solid-state physics and electronics," Phys. Rev. Lett., vol.58, pp.2059–2062, 1987.

[2] O. Painter, R.K. Lee, A. Scherer, A. Yariv, J.D. O'Brien, P.D. Dapkus, and I. Kim, "Two-dimensional photonic band-gap defect mode laser," Science, vol.284, pp.1819–1821, 1999.

[3] S. Noda, K. Tomoda, N. Yamamoto, and A. Chutinan, "Full three-dimensional photonic crystals at near-infrared wavelengths," Science, vol.289, pp.604–606, 2000.

[4] S. Noda, M. Imada, and A. Chutinan, "Trapping and emission of photons by a single defect in a photonic bandgap structure," Nature, vol.407, pp.608–610, 2000.

[5] B.S. Song, S. Noda, and T. Asano, "Photonic devices based on in-plane hetero photonic crystals," Science, vol.300, p.1537, 2003.

[6] S. Noda and T. Baba, ed., Roadmap on Photonic Crystals, Kluwer Academic, Boston, MA, 2003.

[7] M. Imada, S. Noda, A. Chutinan, T. Tokuda, M. Murata, and G. Sasaki, "Coherent two-dimensional lasing action in surface-emitting laser with triangular-lattice photonic crystal structure," Appl. Phys. Lett., vol.75, pp.316–318, 1999.

[8] M. Imada, A. Chutinan, S. Noda, and M. Mochizuki, "Multidirectionally distributed feedback photonic crystal lasers," Phys. Rev. B, Condens. Matter, vol.65, p.195306, 2002.

[9] S. Noda, M. Yokoyama, M. Imada, A. Chutinan, and M. Mochizuki, "Polarization mode control of two-dimensional photonic crystal laser by unit cell structure design," Science, vol.293, pp.1123–1125, 2001.

[10] M. Yokoayama and S. Noda, "Polarization mode control of two-dimensional photonic crystal laser having a square lattice structure," IEEE J. Quantum Electron., vol.39, pp.1074–1080, 2003.

[11] M. Meier, A. Mekis, A. Dodabalapur, A. Timko, R.E. Slusher, J.D. Joannopoulos, and O. Nalamasu, "Laser action from two-dimensional distributed feedback in photonic crystals," Appl. Phys. Lett., vol.74, pp.7–9, 1999.

[12] K. Inoue, M. Sasada, J. Kawamata, K. Sakoda, and J.W. Haus, "A two-dimensional photonic crystal laser," Jpn. J. Appl. Phys.2, Lett., vol.38, pp.L157–L159, 1999.

[13] M. Meier, A. Dodabalapur, J.A. Rogers, R.E. Slusher, A. Mekis, A. Timko, C.A. Murray, R. Ruel, and O. Nalamasu, "Emission characteristics of two-dimensional organic photonic crystal lasers fabricated by replica molding," J. Appl. Phys., vol.86, pp.3502–3507, 1999.

[14] K.S. Yee, "Numerical solution to initial boundary value problems involving Maxwell's equations in isotropic media," IEEE Trans. Antennas Propag., vol.AP-14, no.3, pp.302–307, 1966.

[15] G. Mur, "Absorbing boundary conditions for the finite-difference approximation of the time-domain electromagnetic-field equations," IEEE Trans. Electromagn. Compat., vol.EMC-23, no.4, pp.377–382, 1981.

[16] J.D. Jackson, Classical Electrodynamics, Wiley, New York, 1962.

[17] O.J. Painter, J. Vuckovic, and A. Scherer, "Defect modes of a two-dimensional photonic crystal in an optically thin dielectric slab," J. Opt. Soc. Am. B, vol.16, pp.275–285, 1999.

[18] T. Ochiai and K. Sakoda, "Dispersion relation and optical transmittance of a hexagonal photonic crystal slab," Phys. Rev. B, Condens. Matter, vol.63, p.125107, 2001.

[19] S. Fan and J.D. Joannopoulos, "Analysis of guided resonances in photonic crystal slabs," Phys. Rev. B, Condens. Matter, vol.65, p.235112, 2002.

Mitsuru Yokoyama was born in Kyoto, Japan on February 27, 1970. He received B.S., and M.S. degrees in electrical engineering from Doshisha University, Kyoto, Japan, in 1992 and 1994, respectively. From 1994 to 1998, he was with Mitsubishi Electric Corporation. In 1998, he joined Minolta Co., Ltd. Since joining Minolta, he has been engaged in research and development on optical wave-guide and optical switch. From 2000 to 2003, he was a Visiting Researcher at Kyoto University and researched the Photonic Crystal Laser. He is a member of the Japan Society of Applied Physics.

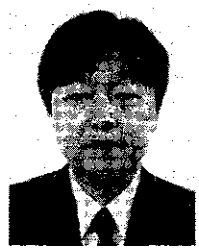

Susumu Noda received B.S., M.S., and Ph.D. degrees all in electronics from Kyoto University, Japan, in 1982, 1984, and 1991, respectively. From 1984 to 1988, he was with Mitsubishi Electric Corporation, and was engaged in research on optoelectronic devices such as AlGaAs/GaAs distributed feedback (DFB) lasers, multiple quantum well (MQW) DFB lasers, and grating-coupled surface-emitting lasers. His Ph.D. thesis summarizes the above works performed at Mitsubishi Electronic Corporation. In 1988, he joined Kyoto University as a research associate and became the associate professor in 1992, and is currently a professor of Department of Electronic Science and Engineering in Kyoto University. His research interest covers quantum optoelectronics field including photonic nanostructures and quantum nanostructures. He has been actively studied ultrafast optical devices using intersubband-transition in quantum wells, growth and characterization of InAs quantum dots on GaAs substrate, and semiconductor-based 3D and 2D photonic crystals. He has an author of more than 200 scientific journals including Nature and Science on these research fields. He received Ando Incentive Prize, Marubun Incentive Prize, IBM Science Award, and Sakurai Award of Optoelectronic Industry and Technology Development Association (OITDA) in 1991, 1999, 2000, and 2002, respectively. He is a member of IEEE and JAPS. He is currently organizing sessions and/or symposiums on photonic nanostructures including photonic crystals in CLEO/QELS, CLEO/PR, MRS, Workshop on Photonics and Electromagnetic Crystal Structures, and so on.